Plasma Physics, Vol. 19, pp. 817 to 838. Pergamon Press, 1977. Printed in Northern Ireland

MACROSCOPIC KINK INSTABILITIES IN TOROIDAL RELATIVISTIC BEAMS*

D. A. SPONG, O. C. ELDRIDGE†
Oak Ridge National Laboratory, Oak Ridge, Tennessee 37830, U.S.A.

and

T. KAMMASH
University of Michigan, Ann Arbor, Michigan, U.S.A.

(*Received* 15 *October* 1976)

Abstract—Applications of relativistic beams in confinement and heating of toroidal plasmas have been discussed in recent years. We have examined the interaction of such beams with the shear Alfvén modes of the background plasma and have found a class of low-frequency instabilities which are similar to the hydrodynamic kink instabilities of a current-carrying plasma. However, for the case of a beam-plasma configuration, the spectrum of the Alfvén modes is, in general, complex, which precludes the use of an energy principle. We employ a normal mode approach and have calculated both growth rates and real frequencies for $n = 1$, $m = 1, 2, 3, 4$ instabilities for various values of beam energy and v_A/c. We assume a cold model for the background plasma, but do not make the MHD ordering $\omega \ll \omega_{ci}$. A fixed boundary model of the beam-plasma system is employed and effects of energy spread in the beam are discussed.

1. INTRODUCTION

THERE HAS been a continuing interest over the past few years in the use of intense relativistic beams in toroidal fusion configurations such as the Tokamak (HAMMER and PAPADOPOULOS, 1975; MOHRI *et al.*, 1975; BENFORD *et al.*, 1974, GILAD *et al.*, 1974; SWAIN *et al.*, 1975). Some of the motivations behind this application are those of supplementary plasma heating relatively steady-state toroidal currents due to the long classical life-times of high energy electrons; and possibly altered macroscopic stability properties (KNOEPFEL *et al.*, 1976; SPONG *et al.*, 1974; LEE, 1973; LOVELACE, 1976). In this paper we wish to examine the third feature in particular.

Several methods have been suggested for generating and sustaining such beams. One is to externally inject a diode-generated beam; the feasibility of such a scheme is now under examination at a number of laboratories. A primary difficulty to be overcome is the achievement of an efficient process for injecting charged particels across strong magnetic field lines. Techniques which have been suggested involve either a momentary disruption of the magnetic surfaces at the instant of injection (GILAD *et al.*, 1974) or a reliance on single particle drifts to carry the beam into the plasma region (BENFORD *et al.*, 1974; SWAIN *et al.*, 1975).

A second method for creating such a beam is the electron runaway phenomenon—which occurs whenever an electric field is applied to a plasma. It has been observed in several Tokamak experiments (SPONG *et al.*, 1974; VLASEKOV *et al.*, 1973; ALIKAEV *et al.*, 1973; ALIKAEV *et al.*, 1975) that in certain regimes of operation (low density, high impurity), runaway-dominated discharges may be produced where a group of relativistic (1–7 MeV) electrons carries a

* Research sponsored by the Energy Research and Development Administration under contract with Union Carbide Corporation.

† Consultant, University of Tennessee, Knoxville, Tennessee.

substantial portion of the toroidal current. These discharges have indicated a number of interesting features such as anomalous ion heating (ALIKAEV *et al.*, 1975); low levels of externally measured MHD activity (KNOEPFEL *et al.*, to be published; VLASENKOV *et al.*, 1973); high β_p values, indicating a more efficient kinetic energy storage capability than has been obtained in normal Tokamak discharges (KNOEPFEL *et al.*, to be published; ALIKAEV *et al.*, 1975); and enhanced levels of microwave emission, near ω_{ce} and its harmonics (COSTLY *et al.*, 1974). Producing toroidal relativistic beams by the runaway method has the advantage that the electrons do not have to be injected across field lines, but has the possible disadvantage that one may not have the same degree of control over the beam energy and density as would be the case with a diode-generated beam.

In the following sections we examine the macroscopic stability features of a toroidal relativistic beam-plasma configuration against kink modes. The current density in conventional Tokamak discharges is typically thought to be limited by the onset of external kink instabilities at the Kruskal–Shafranov limit ($q = rB_t/R_0B_\theta = 1$). The examination of such instabilities is of importance for toroidal relativistic beams due to the potentially high current densities which may be carried ($j \simeq 50\,\mathrm{kA/cm^2}$ per $10^{13}\,\mathrm{cm^{-3}}$ of beam density). As mentioned above, there have been several observations that the externally measured MHD activity of Tokamak runaway discharges is at a somewhat lower level than in normal discharges (KNOEPFEL *et al.*, to be published; VLASENKOV *et al.*, 1975). Also, a parameter study (SPONG *et al.*, 1974) made of such discharges has suggested that q may be attaining values less than unity near the central region of the discharge (where the runaway beam was assumed to localized) without complete loss of confinement due to kink instabilities. Although it must be kept in mind that such observations are at present somewhat speculative and are in a highly preliminary stage, they provide motivation for examining possible differences between the gross stability features of a Tokamak configuration in which the toroidal current is carried by low energy conduction electrons and of one in which relativistic electrons carry most of the current. Clearly, since the fusion power density in a Tokamak reactor scales inversely as q^4, there is substantial reason to consider carefully alternative methods of operating Tokamaks which might allow the Kruskal–Shafranov limit to be exceeded.

Kink instabilities in toroidal relativistic beams were first treated by LEE (1973) who performed a normal mode analysis of these instabilities in a cylindrical geometry. The toroidicity was introduced by means of periodic boundary conditions on the perturbed fields. LEE (1975) found that the stability boundary for the beam against $m = \pm 1$, $n = 1$ kink modes corresponded to the condition of closed particles orbits as opposed to the more conventional condition of closed field lines. Since the particle orbits lag slightly behind field lines (due to the finite particle inertia) this condition is somewhat relaxed from the usual $q = 1$ limit. However, in order to allow substantial improvement over this limit for moderate sized Tokamaks and magnetic fields, very high beam energies are required and synchrotron losses would be prohibitive.

More recently, LOVELACE (1976) has also treated the problem of kink instabilities in toroidal relativistic beams by means of an energy principle. He concluded that the stability conditions for kink modes ($m \neq 0$, $n \neq 0$) of the beam

are identical to those of a conventional plasma pinch provided the plasma pressure is replaced with $p(r) = (B^2/8\pi)\beta_t$ where β_t is the ratio of the directed beam kinetic energy density to the toroidal magnetic field (B_t) energy density. His result, in contrast to that of LEE (1973), would then indicate that raising the beam kinetic energy makes the system less stable.

In the following analysis, we consider several effects which were not taken into account in the earlier work and which may be of particular relevance to runaway discharges in present sized Tokamaks. One such effect is the high transit frequency of relativistic electrons (i.e. the frequency at which they move around a flux surface); this can typically be on the order of or greater than the ion cyclotron frequency. This condition leads one to consider a model for the background plasma other than the MHD approximation (which assumes $\omega \ll \Omega_{ci}$) employed by LEE (1973) and LOVELACE (1976). An analogous situation has been found to occur in mirror-confined hot electron plasma and has been examined by GUEST *et al.* (1975) for the case of ballooning modes; the high electron drift frequency was found to have a significant stabilizing influence on such modes.

A second new feature included in this work is the relative stiffness (parallel mass $= \gamma^3 m_0$, perpendicular mass $= \gamma m_0$) characteristic of high energy electrons towards momentum changes along their direction of propagation. It was recognized some time ago (BLUDMAN *et al.*, 1960) that in the absence of external magnetic fields, this property made relativistic beams much less subject to kink and sausage modes than plasma pinches operating at similar current densities.

Our analysis is based on a normal mode approach; perturbed beam currents are obtained by integrating along the unperturbed particle orbits. The effects of both perturbed electric and perturbed magnetic fields are included in the force equation for the beam. We also do not make the assumption, used in previous work, that the frequency characterizing these modes is only purely real or purely imaginary. This corresponds to keeping terms of order $k_\parallel v_\parallel$ relative to ω in the dispersion relation. The fact that ω is in general a complex number prevents the use of an energy principle and reflects the fact that the operators involved in the beam equation of motion are not self-adjoint. This feature occurs in any plasma system where there is a net flow of one component relative to a second component. Instabilities which are purely growing or damped in the moving frame (ω is imaginary) appear with a superimposed oscillation in the laboratory frame (ω is complex).

Our analysis proceeds according to the following outline. We first discuss the physical model, particle orbits, and perturbed field equations. Next, the perturbed currents for the plasma and beam species are calculated. Substituting these into the perturbed field equations and invoking the appropriate boundary conditions results in a dispersion relation. This is then solved for the cases with no beam (plasma normal modes) and with a beam. In the latter, unstable roots are found and examined with respect to such parameters as beam energy, rotational transform, poloidal mode number and v_A/c.

2. PHYSICAL MODEL, PARTICLE ORBITS, AND FIELD

The model assumed in this work that of a cylindrical relativistic electron beam immersed in a cold background plasma and surrounded by a conducting wall. A

constant magnetic field is applied along the axis of the cylinder; it is assumed that the beam and plasma do not significantly modify this magnetic field, i.e. there is no net diamagnetism or paramagnetism. The effect of toroidicity is introduced by periodic boundary conditions on the perturbed fields. Helical perturbations of the form $\exp[i(m\theta + n\zeta - \omega t)]$, $\zeta = z/R_0$(n, m are integers) are considered. The use of a cold plasma model is justified by the long perpendicular wavelength of the instabilities under consideration. This wavelength is on the order of the plasma minor radius whereas electron and ion Larmor radii are, at most, a few millimeters. Thus, $k_\perp \rho_i$ and $k_\perp \rho_e \ll 1$ and finite Larmor radius corrections for the background plasma are small.

Since a uniform axial current density is assumed, B_θ and q are given by the following:

$$B_\theta(r) = \frac{4\pi}{cr}\int_0^r J(r)r\,\mathrm{d}r = \begin{cases} 2Ir/ca^2 & 0<r<a \\ 2I/cr & r>a \end{cases}, \tag{1}$$

$$q(r) = \frac{rB_z}{R_0 B_\theta} = \begin{cases} q(a) & 0<r<a \\ r^2 B_z c/2R_0 I & r>a \end{cases}, \tag{2}$$

where a = radius of the current channel.

In Cartesian coordinates B_θ may be expressed as

$$B_x = -\frac{yB_z}{qR_0} \qquad B_y = \frac{xB_z}{qR_0}, \tag{3}$$

The unperturbed relativistic orbits are then given by the components of the force equation,

$$\begin{aligned} \frac{\mathrm{d}}{\mathrm{d}t}(\gamma v_x) &= \Omega_e v_y - \frac{\Omega_e x}{qR_0} v_z, \\ \frac{\mathrm{d}}{\mathrm{d}t}(\gamma v_y) &= -\Omega_e v_x - \frac{\Omega_e y}{qR_o} v_z, \\ \frac{\mathrm{d}}{\mathrm{d}t}(\gamma v_z) &= \frac{\Omega_e}{qR_o}(x v_x + y v_y) \simeq 0, \end{aligned} \tag{4}$$

where

$$\Omega_e = \frac{eB_z}{m_0 c}.$$

Since no unperturbed electric field is assumed, γ = constant. Defining $v^\pm = v_x \pm i v_y$, $x^\pm = x \pm iy$ and assuming $x^\pm = x_\perp e^{\pm i\omega t'}$ one obtains from (4) the following equation for ω:

$$\gamma\omega^2 - \Omega_e\omega - \frac{\Omega_e v_z}{qR_o} = 0, \tag{5}$$

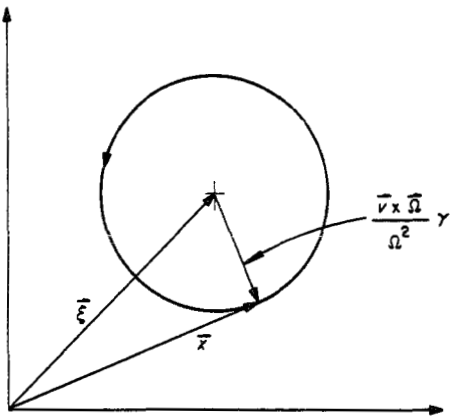

FIG. 1.—Guiding center and gyromotion for a relativistic electron in a magnetic field.

which has the two roots:

$$\omega_+ = \frac{\Omega_e}{2\gamma}[1+\sqrt{1+4v_z\gamma/qR_0\Omega_e}] \simeq \frac{\Omega_e}{\gamma},$$
$$\omega_- = \frac{\Omega_e}{2\gamma}[1-\sqrt{1+4v_z\gamma/qR_0\Omega_e}] \simeq -\omega_{br}\left(1-\frac{2\gamma\omega_{br}}{\Omega_e}\right), \tag{6}$$

where $\omega_{br} = v_z/qR_0 =$ transit or bounce frequency.

ω_+ and ω_- are approximately the gyrofrequency of a relativistic electron and the frequency corresponding to motion along the field lines, respectively. $v^{\pm}$ may be readily calculated by separating out the guiding center motion as indicated in the following equation and in Fig. 1:

$$\boldsymbol{\xi} = \mathbf{x} + \frac{\mathbf{v}\times\boldsymbol{\Omega}}{\Omega^2}\gamma = \mathbf{x} + (\mathbf{v}\times\hat{b})/\omega_+. \tag{7}$$

Here $\boldsymbol{\xi}$ = position of the guiding center. Writing $\boldsymbol{\xi}$ in terms of its Cartesian coordinates and taking time derivates results in the equations

$$\frac{d\xi_x}{dt} = v_x + \frac{1}{\omega_+\gamma}\left[-\Omega_e v_x - \frac{\Omega_e y}{qR_0}v_z\right],$$
$$\frac{d\xi_y}{dt} = v_y - \frac{1}{\omega_+\gamma}\left[\Omega_e v_y - \frac{\Omega_e x}{qR_0}v_z\right]. \tag{8}$$

Combining equations (8), (7) and (5), one obtains the following equation for $\xi^{\pm} = \xi_x \pm i\xi_y$:

$$\frac{d\xi^{\pm}}{dt} = \pm\frac{i\Omega_e v_z}{\omega_+\gamma qR_0}\xi^{\pm} \simeq \mp i\omega_-\xi^{\pm}. \tag{9}$$

Thus $\xi^{\pm} = \xi_{\perp}e^{\pm i(\phi-\omega t)}$ where ϕ is an arbitrary phase factor.

The transverse equations of motion given in (4) may now be written in terms of ξ, the guiding center coordinate, as

$$\frac{\mathrm{d}}{\mathrm{d}t}(\gamma v_x) = \Omega_e v_y - \frac{\Omega_e v_z}{qR_0}(\xi_x - v_y/\omega_+),$$
$$\frac{\mathrm{d}}{\mathrm{d}t}(\gamma v_y) = -\Omega_e v_x - \frac{\Omega_e v_z}{qR_0}(\xi_y + v_x/\omega_+). \tag{10}$$

These may be combined into an equation for $v^{\pm} = v_x \pm iv_y$:

$$\frac{\mathrm{d}v^{\pm}}{\mathrm{d}t} = \mp i\omega_+ v^{\pm} + \omega_+\omega_-\xi^{\pm}. \tag{11}$$

Substituting (9) for $\xi^{\pm}$ one the obtains a solution for $v^{\pm}$,

$$v^{\pm} = v_\perp e^{\pm i(\psi - \omega_+ t)} \mp \frac{i\omega_-\omega_+\xi_\perp e^{i\phi}}{\omega_+ - \omega_-}[e^{\mp i\omega_- t} - e^{\mp i\omega_+ t}]. \tag{12}$$

As may be seen, (12) has components corresponding to both the gyromotion (at ω_+) and the motion along field lines (at ω_-). Note that the frequency ω_- is dependent on the energy $\gamma m_0 c^2$; this is related to the fact that the electrons lag slightly behind field lines due to their finite mass. This dependence will be of importance in the Vlasov treatment which is given in Appendix A. A spreading out in the energy distribution of the relativistic electrons is related to a spreading out in the position of the particle orbits away from field lines.

We now turn to the electromagnetic field equations which are employed in this instability analysis. For perturbed fields with the dependence $\exp[i(m\theta + n\xi - \omega t)]$, the components of Maxwell's curl E and curl B equations (in cylindrical geometry) result in the following six equations:

$$\frac{1}{\rho}\frac{\partial}{\partial\rho}(\rho E_\theta) - \frac{im}{\rho}E_r = iB_z, \tag{13}$$

$$\frac{m}{\rho}E_z - n_\parallel E_\theta = B_r, \tag{14}$$

$$n_\parallel E_r + i\frac{\partial E_z}{\partial\rho} = B_\theta \tag{15}$$

$$\frac{i}{\rho}\frac{\partial}{\partial\rho}(\rho B_\theta) + \frac{m}{\rho}B_r = E_z + \frac{4\pi i J_z}{\omega}, \tag{16}$$

$$-\frac{m}{\rho}B_z + n_\parallel B_\theta = E_r + \frac{4\pi i J_r}{\omega}, \tag{17}$$

$$-n_\parallel B_r - i\frac{\partial B_z}{\partial\rho} = E_\theta + \frac{4\pi i J_\theta}{\omega}, \tag{18}$$

where $\rho = r\omega/c$ and $n_\parallel = nc/R_0\omega$.

In the following instability analysis, these equations are combined in the following manner: B_r and B_θ from (14) and (15) are substituted into (17) and (18)

to obtain equations for E_r and E_θ and terms of E_z, B_z, J_r and J_θ. These are then substituted into (13) and (16) resulting in two differential equations for the perturbed longitudinal fields E_z and B_z:

$$\nabla_\perp{}^2 B_z + (1 - n_\parallel{}^2) B_z = \frac{4\pi}{\omega\rho}\left[i\omega J_r - \frac{\partial}{\partial\rho}(\rho J_\theta)\right], \tag{19}$$

$$\nabla_\perp{}^2 E_z + (1 - n_\parallel{}^2) E_z = -\frac{4\pi i}{\omega}\left\{(1 - n_\parallel{}^2) J_z + \frac{n_\parallel}{\rho}\left[i\frac{\partial}{\partial\rho}(\rho J_r) - m J_\theta\right]\right\}, \tag{20}$$

where

$$\nabla_\perp{}^2 = \frac{1}{\rho}\frac{\partial}{\partial\rho}\rho\frac{\partial}{\partial\rho} - \frac{m^2}{\rho^2}.$$

The remaining task is to determine the perturbed currents δJ in terms of the perturbed fields E_z and B_z; this is done in Section 3. Since δJ will generally depend on both longitudinal and transverse components of $\mathbf{E}$ and $\mathbf{B}$, it is necessary to use (14), (15), (17) and (18) to express δJ in terms of E_z and B_z. Once J_r and J_θ are specified, the transverse electric fields are obtained (in terms of E_z and B_z) by solving the equations

$$\frac{4\pi i}{\omega} J_r + (1 - n_\parallel{}^2) E_r = -\frac{m}{\rho} B_z + i n_\parallel \frac{\partial E_z}{\partial\rho}, \tag{21}$$

$$\frac{4\pi i}{\omega} J_\theta + (1 - n_\parallel{}^2) E_\theta = -\frac{m n_\parallel}{\rho} E_z - i\frac{\partial B_z}{\partial\rho}. \tag{22}$$

When $\mathbf{J} = 0$ (no plasma or beam), the two equations reduce to the usual waveguide *TM* and *TE* equations as given for example, in JOHNSON (1965). Once two coupled eigenmode equations are obtained for E_z and B_z from (19) and (20), solution and application of appropriate boundary conditions results in a dispersion relation. This will be worked out in Section 4 for a fixed boundary model.

In the previous work on kink instabilities the coupling between (19) and (20) has been neglected. LOVELACE (1976) assumes $\delta\mathbf{E}\cdot\mathbf{B} = 0$ whereas LEE (1973) neglects all perturbed electric fields. These approximations are related to the assumption of a highly conducting plasma and result in consideration only of (19) (or its equivalent in terms of vector potential δA_θ) with J_r and J_θ expressed in terms of δB_z (or δA_θ).

3. PERTURBED CURRENTS

Background plasma

The dynamics of the electrons and ions in the background plasma are described by the force equations

$$\frac{\mathrm{d}v_{e,i}^{\pm}}{\mathrm{d}t} = \mp i\Omega_{e,i} v_{e,i}^{\pm} - \frac{v_{ze,i}\Omega_{e,i} x_{e,i}^{\pm}}{qR_0} + \frac{e}{m_{e,i}} E^{\pm}, \tag{23}$$

$$\frac{\mathrm{d}v_{ze,i}}{\mathrm{d}t} = \frac{\Omega_{e,i}}{qR_0}\frac{\mathrm{d}}{\mathrm{d}t}\left(\frac{r^2}{2}\right) + \frac{e}{m_{e,i}} E_z. \tag{24}$$

The orbits of the electrons and ions are

$$v_{e,i}^{\pm} = v_{\perp} e^{\pm i(\psi - \omega_+ t)} \mp \frac{i\omega_+ \omega_-}{\omega_+ + \omega_-} \xi_{\perp} e^{\pm i\theta_0} [e^{\pm i\omega_- t} - e^{\pm i\omega_+ t}], \tag{25}$$

$$v_{e,i}^{z} = \frac{\Omega_{e,i} r^2}{2qR_0} + v_{\parallel}, \tag{26}$$

where $v_{\parallel}$, $v_{\perp}$, θ_0, $\xi_{\perp}$ = initial conditions.

ω_+ and ω_- are the non-relativistic analogues of the frequencies defined in (6). Since the analysis here is for a cylinder with a constant magnetic field, it will not include certain effects which occur in a toroidal geometry. These include the trapping of electrons and ions which mirror on the high field side of the cross section. Such effects will be ignored since they are of importance for kilocycle frequencies, but not for megacycle frequencies near the Alfvén transit frequency. The guiding center for the above orbits is defined by

$$\xi_x = x + \frac{v_y}{\omega_+}, \qquad \xi_y = y - \frac{v_x}{\omega_+} \tag{27}$$

and has the time dependence $\xi^{\pm} = \xi_{\perp} e^{\pm i(\theta - \omega_- t)}$.

Given the above unperturbed orbits, one may calculate perturbed velocities by retaining the perturbed electric field terms in (23) and (24). The following dependence has been assumed for the perturbed fields:

$$\begin{aligned} E^{\pm} &= E_x \pm iE_y \\ &= [\varepsilon_r(r) \pm i\varepsilon_\theta(r) \exp i[(m \pm 1)\theta + nz/R_0 - \omega t]. \end{aligned} \tag{28}$$

Since only long wavelength modes are of interest in this work, it is assumed that ε_r and ε_θ are slowly varying functions of r (in comparison to a gyroradius). Such an ordering implies that the r and θ positions of plasma electrons and ions are essentially constant over the time scale of the instability. The only variation in position allowed is that due to gyromotion, the bounce motion is neglected since it is on a much slower time scale than that characterizing the instability. Under the above approximations, the perturbed plasma currents are given by

$$4\pi J_{e,i}^{\pm} = \frac{i\omega_{pe,i}^2 E^{\pm}}{\omega \mp \Omega_{e,i}}, \qquad 4J_{ze,i} = -\frac{i\omega_{pe,i}^2 E_z}{\omega}. \tag{29}$$

In the case of electrons, we neglect ω in comparison with Ω_e; however, as mentioned earlier, Ω_i is retained in comparison to ω since these frequencies are not necessarily far separated.

Relativistic beam perturbed currents

The starting point for calculating the perturbed beam currents is the relativistic

force equation; the Cartesian components of t equation are given by

$$\frac{\mathrm{d}}{\mathrm{d}t}(\gamma v_x) = \Omega_e v_y - \frac{\Omega_e v_z x}{qR_0} - \frac{e}{m_0}\left(+ \frac{v_y B_z - v_z B_y}{c}\right),$$

$$\frac{\mathrm{d}}{\mathrm{d}t}(\gamma v_y) = -\Omega_e v_x - \frac{\Omega_e v_z y}{qR_0} - \frac{e}{m_0}\left(+ \frac{v_z B_x - v_x B_z}{c}\right), \tag{30}$$

$$\frac{\mathrm{d}}{\mathrm{d}t}(\gamma v_z) = -\frac{\Omega_e}{qR_0}(x v_x + y v_y) - \left(E_z + \frac{v_x B_y - v_y B_x}{c}\right).$$

Here the fields E_x, B_x, ... are perturbed fiel the equilibrium fields are con- tained in Ω_e and q. In the following analysis e terms arising from transverse beam velocities crossed into the longitudinal transverse perturbed magnetic fields are neglected. Such terms are expecte be down by an order $(qA)^{-1}$ (A = aspect ratio) from those retained. We ll also average the perturbed equations of motion over the gyromotion, i.e. drift approximation is used. A final assumption is that all non-linear terms n be neglected.

It will be recalled from Section 1 that the perturbed guiding center orbits are

$$\begin{aligned} v_x &= -\omega_{br} y, \\ v_y &= \omega_{br} x, \\ \frac{\mathrm{d}}{\mathrm{d}t}(\gamma v_z) &= -\frac{\Omega_e}{qR_0}(-\omega_{br} xy \quad \omega_{br} xy) = 0. \end{aligned} \tag{31}$$

The Cartesian coordinates of the unperturbed bits are then given by

$$\begin{aligned} x &= r\cos(\theta_0 + \omega \\ y &= r\sin(\theta_0 + \omega \\ z &= z_0 + v_\parallel t. \end{aligned} \tag{32}$$

The first order perturbed beam velocities are

$$\begin{aligned} v_x &= -\omega_{br} y - \frac{e}{m_0 \Omega_e}\left(E \quad \frac{v_z}{c} B_x\right), \\ v_y &= \omega_{br} x + \frac{e}{m_0 \Omega_e}\left(E_x - \quad B_y\right), \\ \frac{\mathrm{d}}{\mathrm{d}t}(\gamma v_z) &= -\frac{e}{m_0} E_z. \end{aligned} \tag{33}$$

Also, from the relativistic energy equation, o has

$$\frac{\mathrm{d}\gamma}{\mathrm{d}t} = -\frac{e}{m_0 c^2} v_z \tag{34}$$

The perturbed velocities in the longitudinal and transverse directions are then obtained by integrating equations (33) and (34) with respect to time over the unperturbed orbits. First, for the perturbed velocity in the z direction,

$$\delta(\gamma v_z) = \gamma \delta v_z + v_\parallel \delta\gamma = -\frac{e}{m_0}\int_{-\infty}^{t} dt' E_z(t') = -\frac{ieE_z}{m_0[\omega-(m+nq)\omega_{br}]} \tag{35}$$

is obtained.

Also, integrating the energy equation (34) results in

$$\delta\gamma = -\frac{iev_\parallel E_z}{m_0 c^2[\omega-(m+nq)\omega_{br}]}. \tag{36}$$

Combining (35) and (36) then gives the perturbed longitudinal velocity,

$$\delta v_z = \frac{-ieE_z}{m_0\gamma^3[\omega-(m+nq)\omega_{br}]}. \tag{37}$$

In order to obtain the perturbed transverse velocities from equations (33) it is necessary to first calculate the perturbed positions; these may be found by integrating the first two equations of (33). Written in terms of $x^\pm$ and $v^\pm$, these are given by

$$v^\pm = \frac{dx^\pm}{dt} = \pm i\omega_{br}x^\pm - \frac{e}{m_0\Omega_e}\left(\mp iE^\pm + \frac{v_z}{c}B^\pm\right). \tag{38}$$

Equation (38) has the solution

$$x^\pm = re^{\pm i(\theta_0+\omega_{br}t)} + \delta x^\pm. \tag{39}$$

The perturbed position $\delta x^\pm$ is obtained by integrating over the unperturbed orbits and is given by

$$\delta x^\pm = \pm\frac{e(E^\pm \pm iV_zB^\pm/c)}{m_0\Omega_e[\omega-(m+nq)\omega_{br}]}. \tag{40}$$

Substituting the above result back into (38) leads to the desired transverse perturbed velocities,

$$v^\pm = v_\perp e^{\pm i(\theta_0+\omega_{br}t)} + \delta v^\pm,$$

where

$$\delta v^\pm = \mp\frac{ie}{m_0\Omega_e}(E^\pm \pm iv_zB^\pm/c)\left[1\mp\frac{\omega_{br}}{\omega-(m+nq)\omega_{br}}\right]. \tag{41}$$

Now that the perturbed velocities have been calculated, perturbed beam currents may be found. The perturbed distribution function is given by

$$\delta f = F_0(v_\perp, v_\parallel, r) - \delta v_\perp\frac{\partial F_0}{\partial v_\perp} - \delta v_\parallel\frac{\partial F_0}{\partial v_\parallel} - \delta r\frac{\partial F_0}{\partial r}. \tag{42}$$

For the case of a beam of relativistic electrons with uniform velocity near the speed of light and no transverse thermal energy, an appropriate distribution function is $F_0 = \delta(v_z - v_0)\delta(v_\perp - r\omega_{br})$ where $v_0 \simeq c$. The perturbed currents in this

case are given by

$$4\pi J^{\pm} = \pm\frac{i\omega_{pb}^2}{\Omega_e}(E^{\pm} \pm iv_z B^{\pm}/c)\left[1 \mp \frac{\omega_-}{\omega-(m+nq)\omega_{br}}\right], \tag{43}$$

$$4\pi J_z = \frac{i\omega_{pb}^2}{\gamma^3}\frac{E_z}{\omega-(m+nq)\omega_{br}} + \frac{iv_z}{\Omega_e}\frac{\partial}{\partial r}(\omega_{pb}^2)\frac{E_\theta + B_r}{\omega-(m+nq)\omega_{br}} \tag{44}$$

where

$$\omega_{pb}^2 = \frac{4\pi n_b e^2}{m_0}.$$

The final term in (44) arises from the integral $\int 4\pi e d^3v\, \delta r v_z \partial F_0/\partial r$. A uniform density profile is assumed in the following analysis so that this last term of J_z will be absent. If one wished to examine the case in which the beam density was still uniform, but localized within the plasma at a radius r_b, then the final term of (44) would contribute a Dirac delta function $\delta(r-r_b)$ to the perturbed J_z. This is physically due to the perturbed surface current caused by the gross motion of the beam boundary as it is undergoing displacement. In this situation, boundary conditions on the perturbed fields at $r = r_b$ must be derived by multiplying the two coupled equations (19) and (20) by rdr and integrating over the layer $r_b - \varepsilon$ to $r_b + \varepsilon$ with $\varepsilon \to 0$.

For the case in which the relativistic beam has an energy spread, a Vlasov approach must be employed in calculating perturbed currents. This approach is presented in Appendix A.

4. DISPERSION RELATION DERIVATION

A dispersion relation is derived for the case of a fixed boundary beam-plasma model (beam and plasma extend all the way to a conducting wall). For simplicity, the perturbed beam currents derived in Section 3 will be used; the derivation could readily be generalized to the case of the Vlasov beam model given in Appendix A. The derivation is made according to the following outline. First, the perturbed currents for the three species present, electrons, ions, beam electrons, are substituted into the field equations of Section 2. Next, these equations are manipulated until two coupled equations for the perturbed fields E_z and B_z are obtained. Finally, a method for decoupling these equations is used and a dispersion relation is obtained by requiring the appropriate boundary conditions to be satisfied by E_z and B_z.

Adding up the perturbed currents for the three species as given by (29), (38) and (39) results in the following currents:

$$\frac{4\pi J_r}{\omega} = \frac{i\omega_{pi}^2}{\omega^2-\Omega_i^2}E_r - \frac{\omega_{pi}^2\omega}{(\omega^2-\Omega_i^2)\Omega_i}E_\theta - \frac{i\omega_{pb}^2\omega_{br}[E_r - v_z B_\theta/c]}{[\omega-(m+nq)\omega_{br}]}, \tag{45}$$

$$\frac{4\pi J_\theta}{\omega} = \frac{i\omega_{pi}^2}{\omega^2-\Omega_i^2}E_\theta + \frac{\omega_{pi}^2\omega}{(\omega^2-\Omega_i^2)\Omega_i}E_r - \frac{i\omega_{pb}^2\omega_{br}[E_\theta + v_z B_r/c]}{\omega\Omega_e[\omega-(m+nq)\omega_{br}]}, \tag{46}$$

$$\frac{4\pi J_z}{\omega} = \frac{i\omega_{pe}^2}{\omega^2}E_z + \frac{i\omega_{pb}^2}{\omega\gamma^3}\frac{E_z}{[\omega-(m+nq)\omega_{br}]}. \tag{47}$$

The field (14) and (15) are used for B_r and B_θ; also, the following quantities are defined:

$$Q = \frac{\omega_{br}\omega_{pb}^2}{\epsilon[\omega-(m+nq)\omega_{br}]}, \tag{48}$$

$$= \frac{\omega\omega_{pi}^2}{\Omega_i(\omega^2-\Omega_i^2)}, \tag{49}$$

$$= 1-\frac{\omega_{pi}^2}{\omega^2-\Omega_i^2}, \tag{50}$$

$$P = 1-\frac{\omega}{\epsilon} - \frac{\omega_{pb}^2}{\omega\gamma^3[\omega-(m+nq)\omega_{br}]}. \tag{51}$$

The perturbed currents (45)–(47) may then be written in the form

$$\frac{4\pi i J_r}{\omega} = [S-1-n_\parallel)Q]E_r - iDE_\theta - iQ\frac{\partial E_z}{\partial\rho}, \tag{52}$$

$$\frac{4\pi i J_\theta}{\omega} = [S-1-n_\parallel)Q]E_\theta + iDE_r + iQ\frac{\partial E_z}{\partial\rho}, \tag{53}$$

$$\frac{4\pi i J_z}{\omega} = (P-1 \quad .. \tag{54}$$

The transverse perturbed electric fields, E_r and E_θ, are now obtained in terms of E_z and B_z by substituting J_r and J_θ, as given above, into (21) and (22). It is convenient to define the following quantities:

$$\varepsilon_1 = \epsilon \quad [S-n_\parallel^2+(1-n_\parallel)Q], \tag{55}$$

$$\varepsilon \quad = G^{-1}D(n_\parallel+Q), \tag{56}$$

$$\varepsilon_3 = 1+G^{-1} \quad n_\parallel+Q)[S-n_\parallel^2+(1-n_\parallel)Q], \tag{57}$$

$$\varepsilon_4 = n_\parallel DG^{-1} \tag{58}$$

$$G = [\quad n_\parallel^2+(1-n_\parallel)Q]^2-D^2. \tag{59}$$

E_r and E_θ are then obtained, as

$$E_r = \frac{i}{n_\parallel}(\varepsilon_3-1 \quad -\frac{m}{\rho}\varepsilon_1 B_z + \frac{\varepsilon_4}{n_\parallel}\frac{\partial B_z}{\partial\rho} - \frac{im}{\rho}\varepsilon_2 E_z, \tag{60}$$

$$E_\theta = -i\varepsilon_1\frac{\partial B_z}{\partial\rho} - \quad (\varepsilon_3-1)E_z + \varepsilon_2\frac{\partial E_z}{\partial\rho} + \frac{im}{\rho n_\parallel}\varepsilon_4 B_z. \tag{61}$$

Substituting the above equations into (13) results in the equation

$$\varepsilon_1\nabla_\perp^2 \quad + B_z + i\varepsilon_2\nabla_\perp^2 E_z = 0, \tag{62}$$

where

$$\nabla_\perp \quad = \frac{1}{\rho}\frac{\mathrm{d}}{\mathrm{d}\rho}\left(\rho\frac{\mathrm{d}}{\mathrm{d}\rho}\right) - \frac{m^2}{\rho^2}.$$

This is the first of two coupled radial eigenvalue equations whose eigenvalues determine the growth rates of the unstable modes. Combining (14), (15) and (16) with equations (60) and (61) for E_r and E_θ then results in the second of the two coupled equations,

$$\varepsilon_3 \nabla_\perp{}^2 E_z + P E_z - i\varepsilon_4 \nabla_\perp{}^2 B_z = 0. \tag{63}$$

In order to examine stability, it is necessary to find eigenvalues of the coupled system of (62) and (63). These may be put into a somewhat more convenient form by multiplying (62) by $-\varepsilon_3/\varepsilon_2$, adding to (63), and then multiplying (63) by $-i\varepsilon_1/\varepsilon_4$ and adding to (62). This results in the two coupled equations

$$(\nabla_\perp{}^2 + T_B{}^2) B_z = T_{BE}{}^2 E_z, \tag{64}$$

$$(\nabla_\perp{}^2 + T_E{}^2) E_z = T_{EB}{}^2 B_z, \tag{65}$$

where

$$T_B{}^2 = \varepsilon_3/(\varepsilon_1\varepsilon_3 - \varepsilon_2\varepsilon_4),$$
$$T_E{}^2 = \varepsilon_1 P/(\varepsilon_1\varepsilon_3 - \varepsilon_2\varepsilon_4),$$
$$T_{BE}{}^2 = iP\varepsilon_2/(\varepsilon_1\varepsilon_3 - \varepsilon_2\varepsilon_4),$$
$$T_{EB}{}^2 = -i\varepsilon_4/(\varepsilon_1\varepsilon_3 - \varepsilon_2\varepsilon_4).$$

A technique for decoupling equations of the form (64) and (65) has been given in JOHNSON (1965). The solutions are

$$E_z = \frac{Z_1\psi_2 - Z_2\psi_1}{Z_1 - Z_z}, \tag{66}$$

$$B_z = \frac{\psi_1 - \psi_2}{Z_1 - Z_2}, \tag{67}$$

where

$$\psi_1 = A_1 J_m(T_1\rho),$$
$$\psi_2 = A_2 J_m(T_2\rho),$$
$$T_{1,2}^2 = T_E{}^2 - Z_{1,2} T_{BE}{}^2,$$
$$Z_{1,2} = \frac{T_E{}^2 - T_B{}^2}{2T_{BE}{}^2}\left[1 \pm \sqrt{1 + \frac{4T_{BE}{}^2 T_{EB}{}^2}{(T_E{}^2 - TB^2)^2}}\right].$$

A_1 and A_2 are constants which are determined by the boundary conditions.

As mentioned earlier, in the fixed boundary model both the beam and plasma extend all the way to the wall and there is no vacuum region in between. The wall is assumed to be perfectly conducting, so that the following requirements must be satisfied by the perturbed fields:

$$E_z(\rho_a) = E_\theta(\rho_a) = B_r(\rho_a) = 0, \tag{68}$$

where $\rho_a = a\omega/c$, a = shell radius.

Setting E_z equal to zero at the boundary (using equations 66) leads to the equation

$$A_1 = \frac{Z_1}{Z_2} A_2 \frac{J_m(T_2\rho_a)}{J_m(T_1\rho_a)}. \tag{69}$$

Next, using (61) and setting E_θ to zero at $\rho = \rho_a$ leads to the equation

$$-i\varepsilon_1 \frac{\partial B_z}{\partial \rho}\bigg|_{r=a} + \varepsilon_2 \frac{\partial E_z}{\partial \rho}\bigg|_{r=a} + \frac{im}{\rho_a n_\parallel} \varepsilon_4 B_z \bigg|_{r=a} = 0 \tag{70}$$

Substituting (66) and combining with (69) results in the desired dispersion relation,

$$Z_2 T_2 (i\varepsilon_1 + \varepsilon_2 Z_1) \frac{J_m'(\rho_a T_2)}{J_m(\rho_a T_2)} - Z_1 T_1 (i\varepsilon_1 + \varepsilon_2 Z_2) \frac{J_m'(\rho_a T_1)}{J_m(\rho_a T_1)} + \frac{im\varepsilon_4}{\rho_a n_\parallel} (Z_1 - Z_2) = 0. \tag{71}$$

5. NORMAL PLASMA ALFVÉN MODES

Before examining the unstable spectra (presented in Section 6), the roots of the fixed boundary dispersion relation are obtained (equation (66)) with the relativistic beam density set equal to zero. It can be shown that in this case only

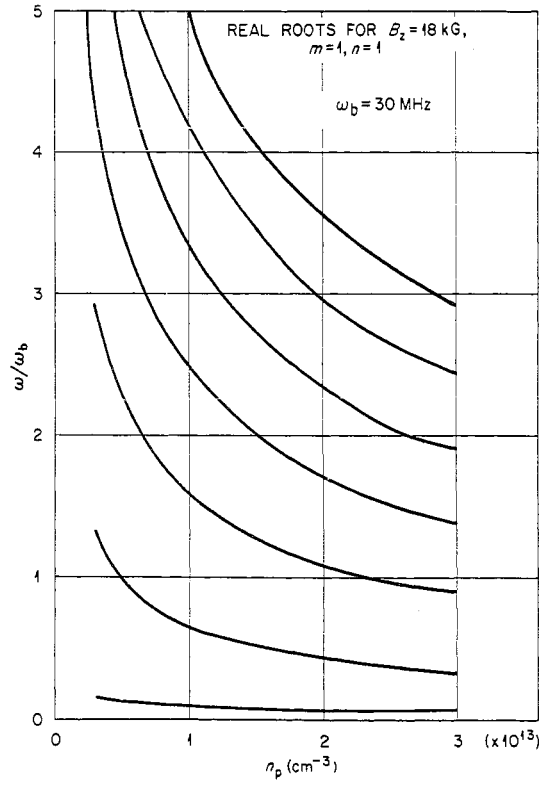

FIG. 2.—Roots of the fixed boundary dispersion relation vs. n_p with $b_B = 0$ and at a fixed B_z.

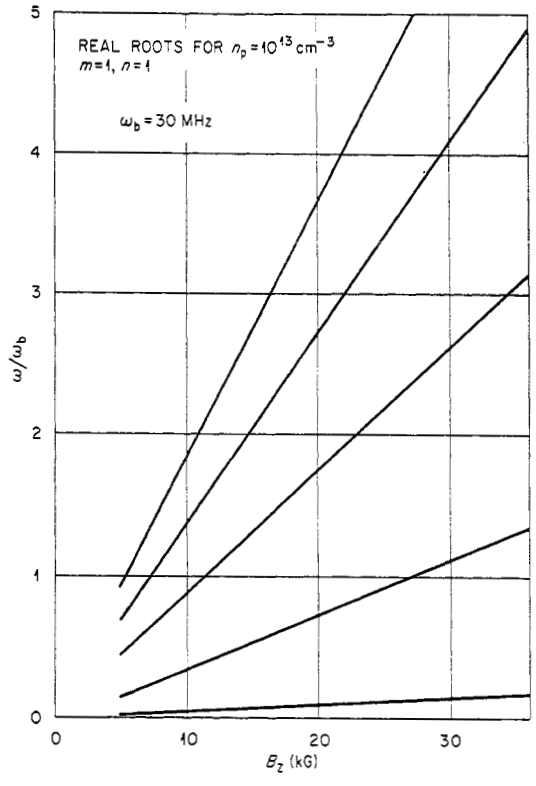

FIG. 3.—Roots of the fixed boundary dispersion relation vs. B_z with $n_B = 0$ and at a fixed n_p.

purely real roots are possible and that these correspond to the Alfvén waves of a cylindrical cavity.

In Figs 2 and 3 roots of the dispersion relation (66) are plotted as functions of plasma density (at fixed toroidal field) and toroidal field (at fixed plasma density). As may be seen, the frequencies do scale with the Alfvén velocity; they vary linearly in magnetic field strength and are inversely proportional to the square root of the plasma density.

By examining the relative sizes of the terms in equation (71) with the beam density equal to zero, some approximate analystic results may be obtained to explain the curves of Figs 2 and 3. The exact dispersion relation is given by

$$Z_2\rho_a T_1^2 T_2 \frac{J_m'(\rho_a T_2)}{J_m(\rho_a T_2)} - Z_1\rho_a T_1 T_2^2 \frac{J_m'(\rho_a T_1)}{J_m(\rho_a T_1)} + \frac{DP}{S+Q} m(Z_1 - Z_2) = 0. \qquad (72)$$

With the beam density equal to zero and for plasma densities, toroidal fields, and minor radii typical of Tokamaks, the first term in the above equation is 4–5 orders of magnitude lower than the other two; also, Z_2 is several orders of magnitude less than Z_1. Thus (72) is adequately approximated by the dispersion relation

$$-\rho_a T_1(S - n_\parallel^2) J_m'(\rho_a T_1) + mDJ_m)(\rho_a T_1) = 0. \qquad (73)$$

Also, for the frequency range of interest ($\omega \lesssim \Omega_{ci}$) the following approximations

may be made:

$$S - n_{\|}^2 \simeq S,$$
$$T_1^2 \simeq c^2/v_A^2, \tag{74}$$
$$D/S \simeq -\omega/\Omega_i.$$

Defining the quantities

$$x = a\omega/v_A,$$
$$\delta = c/a\omega_{pi}, \tag{75}$$

The above dispersion relation may be written as

$$J_{m-1}(x) + m\left(\delta - \frac{1}{x}\right)J_m(x) = 0. \tag{76}$$

Zeros of this equation as a function of the parameter δ have been calculated numerically in SPONG (1976) for $m = 1$ and $m = 2$. It was found that for values of δ characteristic of Tokamaks, the zeros of (76) do not depend strongly on δ and are approximately equal to the zeros of J_{m-1}. Thus the roots of (72) are $\omega \simeq j_{m-1,s}v_A/a$.

6. NUMERICAL RESULTS FOR GROWTH RATES

Unstable roots for the fixed boundary kink mode dispersion relation have been calculated over a range of parameters which are typical of Tokamak strong runaway discharges. These results are presented and discussed in this section. The roots of (71) were obtained by using the Cauchy root-finding subroutine developed by BEASLEY and MEIER (1974). Some care had to be taken in solving equation (71) due to the branch-cut present near the low frequency roots from the square root involved in computing T_1. This may be avoided, however, by noting that the second term of (71) is an even function of T_1 and thus may be written in a form which depends only on T_1^2.

Dependence on beam energy

In Figs 4–7 growth rates and real frequencies are plotted for beam energies of 250 keV, 500 keV, 1 MeV and 14.5 MeV. The beam is assumed to carry 100% of

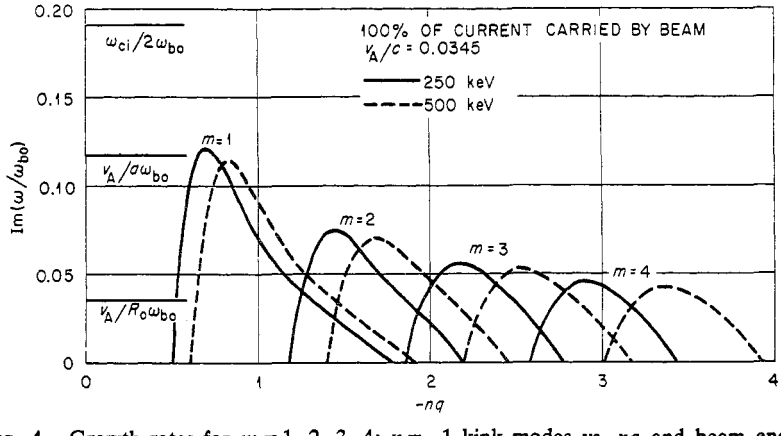

FIG. 4.—Growth rates for $m = 1, 2, 3, 4$; $n = -1$ kink modes vs. nq and beam energy (250, 500 keV) for $v_A/c = 0.0345$.

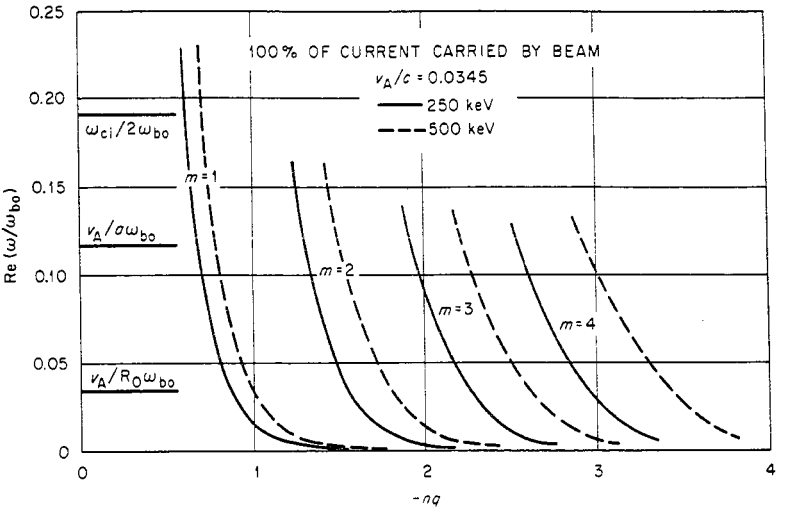

FIG 5.—Real part of the unstable roots for $m = 1, 2, 3, 4,$; $n = -1$ kinks vs. nq and beam energy (250, 500 keV) for $v_A/c = 0.0345$.

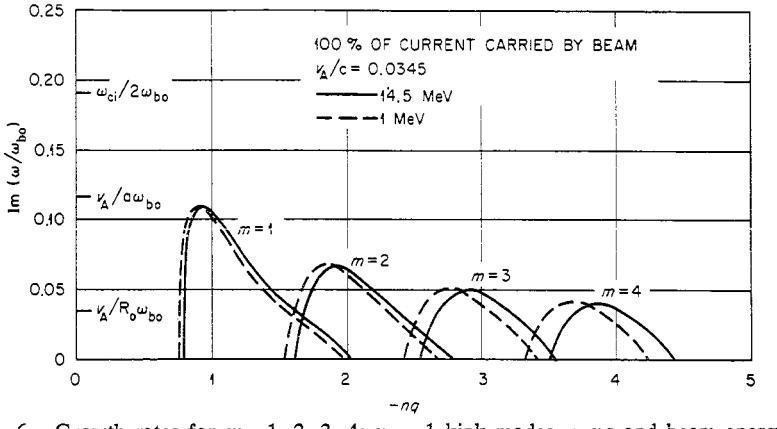

FIG. 6.—Growth rates for $m = 1, 2, 3, 4$; $n = -1$ kink modes vs. nq and beam energy (1, 14.5 MeV) for $v_A/c = 0.0345$.

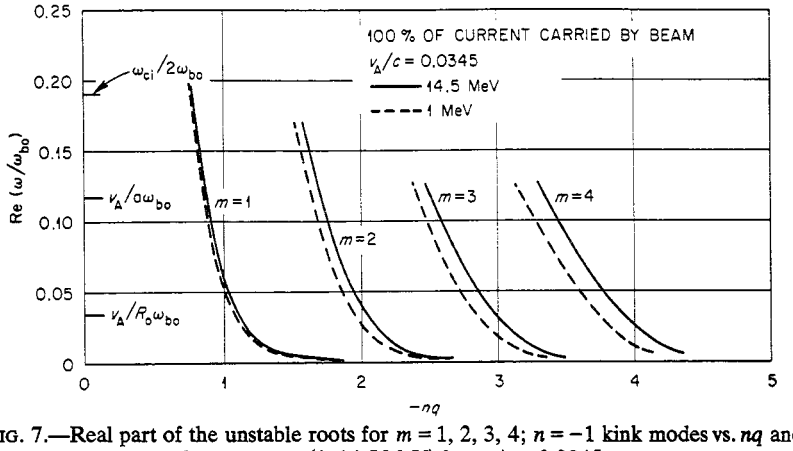

FIG. 7.—Real part of the unstable roots for $m = 1, 2, 3, 4$; $n = -1$ kink modes vs. nq and beam energy (1, 14.5 MeV) for $v_A/c = 0.0345$.

the current and the toroidal field and plasma density are 15 kG and 10^{13} cm^{-3}. Fairly slight differences are present between the 1 MeV and 14.5 MeV cases, but large changes are apparent in going from 250 keV to 500 keV to 1 MeV. Increasing the energy seems to shift the growth rate curves to the right on the q-axis, though not enough to change the shape substantially. This effect is particularly noticeable for the higher m numbers.

Dependence on v_A/c

Growth rates and real frequencies are plotted in Figs 8 and 9 for $v_A/c = 0.058$, 0.042 and 0.034. These correspond to a plasma density of 10^{13} cm^{-3} and toroidal fields of 15, 18 and 25 kG, respectively. The beam is assumed to carry all of the toroidal current and has an energy of 1 MeV. The growth rates appear to be monotonically increasing with v_A/c, as is the case in ideal MHD. It may be noted that the upper value of q where the threshold occurs is relatively independent of v_A/c, whereas the lower threshold is not. The lower marginal point goes to lower values of q as v_A/c is increased.

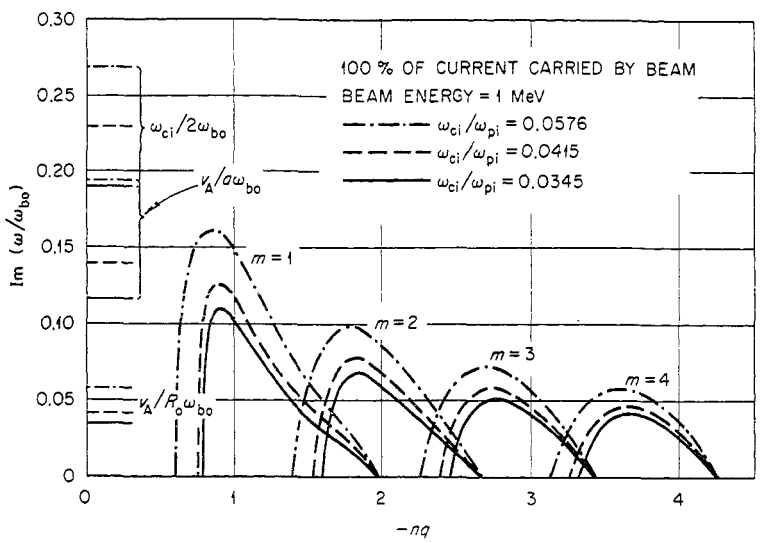

FIG. 8.—Growth rates for $m = 1, 2, 3, 4$; $n = -1$ kink modes vs. nq and ω_{ci}/ω_{pi} for 1 MeV beam energy.

7. CONCLUSIONS

The purpose of this work, as discussed in Section 1, has been to examine the macroscopic stability features of toroidal relativistic beams. A normal mode approach has been taken using a cylindrical geometry with period boundary conditions on the perturbed fields to simulate a torus. The following new features have been included: first the background plasma model has been extended to include frequencies which are not small relative to the ion gyrofrequency. This was motivated by the fact that high energy electrons circulate around flux surfaces at frequencies of the order of Ω_{ci}. Macroscopic modes associated with this component are thus not necessary limited to frequencies $\ll\Omega_{ci}$ as is the case in ideal MHD. Second, both the transverse and longitudinal dynamics of the beam

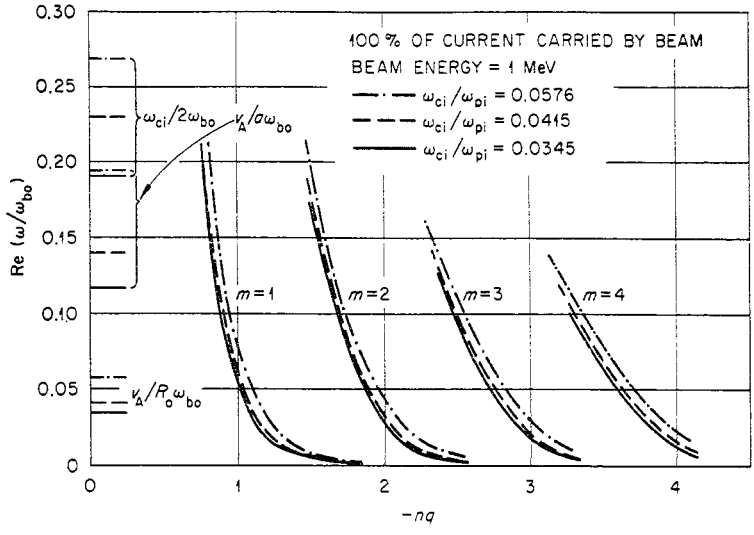

FIG. 9.—Real part of the unstable roots for $m = 1, 2, 3, 4$; $n = -1$ kink modes vs. nq and ω_{ci}/ω_{pi} for 1 MeV beam energy.

electrons are included, whereas previous work has primarily treated the transverse dynamics.

In general, the results for growth rates of kink modes show that maxima occur near the rational magnetic surfaces—as is the case in ideal MHD. However, just to the inside of the rational surface, it was usually observed that the real part of the unstable root rose to high values (up to half of the ion gyrofrequency) while the growth rate dropped rapidly to zero, resulting in stable regions just to the inside of the rational surfaces. We interpret this characteristic as follows. Near the rational q surfaces, the high energy electron orbits are closely aligned with the helical mode structure of the instability which typically grows on a much slower time scale than the drift timescale associated with the fast electrons. Just to the inside of rational q surfaces, the fast electron orbits are no longer in resonance with the instability mode structure. This component can thus connect regions of positive and negative current perturbation just inside the rational surface. Such imbalances may be shorted out by the fast electrons since their poloidal drift frequency is substantially higher that the growth rate of the current perturbations.

A second feature which was observed in these calculations was that the term in the dispersion relation which arises from the longitudinal electron inertia (the first term in equation 66) is typically 4–5 orders of magnitude less than the other terms in the dispersion relation. Thus, at least for the fixed boundary model, it appears that the longitudinal dynamics of the relativistic electrons is not an important factor in determining the growth rates for the instabilities examined here.

In closing, it is noted that this treatment, as well as the previous work (LEE, 1973; LOVELACE, 1976), has been concerned primarily with cylindrical models. The influence of toroidal geometry has been taken into account only by requiring periodic boundary conditions on the perturbed fields. However, there are two other effects which enter in with toroidal geometry and merit further consideration. One is the coupling between various order m modes caused by poloidal variations in beam equilibrium properties. A second effect is large displacements

of the single particle orbits off of flux surfaces when energies become relativistic. These effects are discussed in further detail along with orbit calculations for relativistic electrons in Tokamaks elsewhere (SPONG, 1976).

Acknowledgements—This research was supported by the United States Energy Research and Development Administration and through a Graduate Participantship from Oak Ridge Associated Universities.

REFERENCES

ALIKAEV V. V., ARSENEV Y. I., BOBROVSKII G. A., KOUORARIEV A. A. and RAZUMOVA K. A. (1973) MATT-TRANS-111. Princeton, New Jersey.
ALIKAEV V. V., RAZUMOVA K. A. and SOKOLOV YU. A. (1975) *Sov. J. Plasma Phys.* **1,** 303.
BENSON J., ECKER B. and BAILEY V. (1974) *Phys. Rev. Lett.* **33,** 574.
BEASLEY C. O. and MEIER H. K. (1974 ORNL/TM-4588. Oak Ridge, Tennessee.
BLUDMAN S. A., WATSON K. M. and ROSENBLUTH M. N. (1960) *Physics Fluids* **3,** 747.
COSTLY A. E., HASTIE R. J., PAUL J. W. M. and CHAMBERLAIN J. (1974) *Phys. Rev. Lett.* **33,** 758.
GILAD P., KUSSE B. R. and LOCKNER T. R. (1974) *Phys. Rev. Lett.* **33,** 1275.
GUEST G. E., HEDRICK C. L. and NELSON D. B. (1975) *Physics Fluids* **18,** 871.
HAMMER D. A. and PAPADOUPOLOUS K. (1975) *Nucl. Fusion* **15,** 977.
JOHNSON C. C. (1965) *Field and Wave Electrodynamics.* McGraw-Hill, New York.
KNOEPFEL H., SPONG D. A. and ZWEBEN S. J. (1977) *Physics Fluids* **20,** 511.
LEE E. P. (1973) *Physics Fluids* **16,** 1072.
LOVELACE R. (1976) *Physics Fluids* **19,** 723.
MOHRI A., MASUZAKI M., TSUZUKI T. and IKUTA K. (1975) *Phys. Rev. Lett.* **34,** 574.
SPONG D. A., CLARKE J. F., ROME J. A. and KAMMASH T. (1974) *Nucl. Fusion* **14,** 397.
SPONG D. A. (1976) Ph.D Dissertation. Univ. of Michigan, Ann Arbor, Michigan; ORNL/TM-5147, Oak Ridge, Tennessee.
SWAIN D. W., MILLER P. A. and WIDNER M. M. (1975) SAND 75-0214, Albuquerque, New Mexio.
VLASENKOV V. S., LEONOV V. M., MEREZHKIN V. G. and MUKOHVATOV V. S. (1973) *Nucl. Fusion* **13,** 509.

APPENDIX A

Perturbed beam currents for a beam with energy spread

As was indicated in Section 3, an alternate formulation must be employed in calculating perturbed beam currents when energy spread is present in the relativistic beam. This is presented in the following and is based on the relativistic Vlasov equation.

$$\frac{\partial f}{\partial t}+\mathbf{v}\cdot\nabla f+\frac{e}{m_0}\left[\mathbf{E}+\frac{1}{c}(\mathbf{v}\times\mathbf{B})\right]\cdot\frac{\partial f}{\partial \mathbf{p}}=0. \tag{A.1}$$

where $\mathbf{p}=\gamma m_0\mathbf{v}$ and $\gamma=(1-v^2/c^2)^{-1/2}$.

The above equation is linearized by assuming $f=f_0+\delta f$ where f_0 is an equilibrium distribution function. δf is then obtained by integrating over the characteristic (unperturbed orbits).

$$\delta f=\frac{e}{m_0}\int_{-\infty}^{t}\mathrm{d}t'\left[\mathbf{E}+\frac{\mathbf{v}\times\mathbf{B}}{c}\right]\cdot\frac{\partial f_0}{\partial \mathbf{p}}. \tag{A.2}$$

The equilibrium distribution function f_0 depends only on the three constants of the motion which are given below.

$$H=\gamma m_0c^2,$$
$$P_z=\gamma m_0v_z+\frac{e}{c}A_z,$$
$$L_\theta=\gamma m_0(xv_y-yv_x)+\frac{e}{c}rA_\theta.$$

Expanding $\partial f_0/\partial\mathbf{p}$ by the chain rule allows one to express ∂f as follows.

$$\delta f=\frac{\partial f_0}{\partial H}\delta H+\frac{\partial f_0}{\partial P_z}\delta P_z+\frac{\partial f_0}{\partial L_\theta}\delta L_\theta, \tag{A.4}$$

where

$$\delta H = \int_{-\infty}^{t} \mathrm{d}t'(\mathbf{v}\cdot\delta\mathbf{F}),$$
$$\delta P_z = \int_{-\infty}^{t} \mathrm{d}t'\delta F_z, \tag{A.5}$$
$$\delta L_\theta = \int_{-\infty}^{t} \mathrm{d}t'(x\delta F_y - y\delta F_x).$$

We shall consider equilibrium distribution functions here which depend only on H and P_z, i.e. $f_0 = f_0(H, P_z)$. Using the unperturbed relativistic beam orbits given in Section 2, the time history integrals given in (A.4) may be performed. Assuming that $\omega_+ \gg \omega_-$ (gyrofrequency is much faster than the transit frequency around the torus) results in the equations given below for δP_z and δH.

$$\delta P_z \simeq \frac{ieE_z}{m_0(\omega - \omega_{br}nq - n\omega_-)}. \tag{A.6}$$

$$\delta H \simeq \frac{ie(v_zE_z - r\omega_2E_\theta)}{m_0(\omega - \omega_{br}nq - m\omega_-)} - \frac{ie}{m_0\omega_+}(v_\theta E_r - v_rE_\theta), \tag{A.7}$$

The perturbed relativistic beam current is then given by the following equation.

$$\delta J = -e\int_0^\infty p_\perp dp_\perp \int_0^\infty \mathbf{v}\,\mathrm{d}p_\parallel \left[\delta P_z \frac{\partial f_0}{\partial P_z} + \delta H \frac{\partial f_0}{\partial H}\right]. \tag{A.8}$$

Substituting δP_z and δH from (A.6) and (A.7) into (A.8) and performing an integration by parts on the first term, one obtains the result given below.

$$\delta J = -\omega_{pb}{}^2 \int_0^\infty \rho_\perp \,\mathrm{d}\rho_\perp \int_{-\infty}^\infty \mathrm{d}p_\parallel \mathbf{v}\left\{\frac{1}{m_0}(\omega - \omega_{br}nq - m\omega_-)^{-1},\right.$$
$$\left.\times \frac{f_0}{c\gamma^3}E_z + \frac{1}{c^2}(v_zE_z - r\omega_{br}E_\theta)\frac{\partial f_0}{\partial \gamma}, \quad -\frac{1}{\Omega_e c^2}(v_\theta E_r - v_rE_\theta)\frac{\partial f_0}{\partial \gamma}\right\}.$$

It is more convenient from this point on to convert the above integral to an integration over $v_\parallel$ and γ. The Jacobian of this transformation is given by the following.

$$p_\perp \,\mathrm{d}p_\perp \,\mathrm{d}p_\parallel = p_\perp |J| \,\mathrm{d}v_\parallel \,\mathrm{d}\gamma. \tag{A.10}$$

where

$$|J| = m_0{}^2 v_\perp{}^2 \gamma.$$

In performing the integrations indicated in (A.9) we shall assume a delta function distribution in $v_\parallel$ with a spread allowed in the energy dependence, i.e. $f_0(v_\parallel, \gamma) = \delta(v_\parallel - v_0)F(\gamma)$ where $v_0 \simeq c$. If $\gamma_0 = (1 - v_0{}^2/c^2)^{-1/2}$, then

$$p_\perp |J| = m_0c^2\left(\frac{\gamma^2}{\gamma_0{}^2} - 1\right) \tag{A.11}$$

We shall consider a step function dependence for $F(\gamma)$.

$$F(\gamma) = \begin{cases} 0 & \gamma < \gamma_0, \\ K & \gamma_0 < \gamma < \gamma_m, \\ 0 & \gamma > \gamma_m. \end{cases} \tag{A.12}$$

where K is is a normalization constant.

Substituting the above distribution function into (A.9) then results in the following perturbed currents.

$$\delta J_r = -\frac{2i\omega_{pb}^2}{m_0}\chi(\gamma_0, \gamma_m)\frac{\gamma_0 - \gamma_m}{\omega_+ \gamma_0^2 c^2}E_\theta. \tag{A.13}$$

$$\delta J_\theta = \frac{2i\omega_{pb}^2}{m_0}\chi(\gamma_0, \gamma_m)\frac{\gamma_0 - \gamma_m}{\omega_+ \gamma_0^2 c^2}E_r. \tag{A.14}$$

$$\delta J_z = -\frac{i\omega_{pb}^2}{m_0}\chi(\gamma_0, \gamma_m)\left[\frac{I_1}{\gamma_0^2}E_z - I_2 E_z - \frac{2}{\gamma_0^2 c^2}(cE_z - r\omega_{br}E_\theta)I_3\right] \tag{A.15}$$

where

$$\chi(\gamma_0, \gamma_m) = \frac{3}{2\pi\gamma_0}\left[\frac{\gamma_m^3}{\gamma_0^3} - 3\frac{\gamma_m}{\gamma_0} + 2\right]^{-1}. \tag{A.16}$$

$$I_1 = -[\omega - \omega_{br}(nq+m)]^{-1}\ln\left\{\frac{\gamma_0[\omega - \omega_{br}(nq+m) - \varepsilon m\omega_{br}\gamma_m]}{\gamma_m[\omega - \omega_{br}(nq+m) - \varepsilon m\omega_{br}\gamma_0]}\right\} \tag{A.17}$$

$$I_2 = [\omega - \omega_{br}(nq+m)]^{-1}\left\{\frac{1}{2}\left(\frac{1}{\gamma_0^2} - \frac{1}{\gamma_m^2}\right) + \frac{\varepsilon m\omega_{br}}{\omega - \omega_{br}(nq+m)}\left(\frac{1}{\gamma_0} - \frac{1}{\gamma_m}\right)\right\}$$
$$-\frac{\varepsilon^2 m^2 \omega_{br}^2}{[\omega - \omega_{br}(nq+m)]^3}\ln\left[\frac{\gamma_0[\omega - \omega_{br}(nq+m) - \varepsilon\omega_{br}m\gamma_m]}{\gamma_m[\omega - \omega_{br}(nq+m) - \varepsilon\omega_{br}m\gamma_0]}\right] \tag{A.18}$$

$$I_3 = \frac{\gamma_0 - \gamma_m}{\varepsilon m\omega_{br}} - \frac{\omega - \omega_{br}(nq+m)}{\varepsilon^2 m^2 \omega_{br}^2}\ln\left[\frac{\omega - \omega_{br}(nq+m) - \varepsilon\omega_{br}m\gamma_m}{\omega - \omega_{br}(nq+m) - \varepsilon\omega_{br}m\gamma_0}\right] \tag{A.19}$$

$$\varepsilon = 2\omega_{br}/\Omega_e.$$